

# Flow-Induced Charge Modulation in Superfluid Atomic Fermions Loaded into an Optical Kagome Lattice

Daisuke Yamamoto<sup>1</sup>, Chika Sato<sup>2</sup>, Tetsuro Nikuni<sup>2</sup>, and Shunji Tsuchiya<sup>2</sup>

<sup>1</sup>Condensed Matter Theory Laboratory, RIKEN, 2-1 Hirosawa, Wako, Saitama 351-0198, Japan

<sup>2</sup>Department of Physics, Faculty of Science, Tokyo University of Science,  
1-3 Kagurazaka, Shinjuku, Tokyo 162-8601, Japan

(Dated: November 3, 2018)

We study the superfluid state of atomic fermions in a tunable optical kagome lattice motivated by recent experiments. We show that imposed superflow induces spatial modulations in the density and order parameter of the pair condensate and leads to a charge modulated superfluid state analogous to a supersolid state. The spatial modulations in the superfluid emerge due to the geometric effect of the kagome lattice that introduces anisotropy in hopping amplitudes of fermion pairs in the presence of superflow. We also study superflow instabilities and find that the critical current limited by the dynamical instability is quite enhanced due to the large density of states associated with the flatband. The charge modulated superfluid state can sustain high temperatures close to the transition temperature that is also enhanced due to the flatband, and is therefore realizable in experiments.

PACS numbers: 03.75.Ss, 67.85.-d, 71.10.Fd

Geometric frustration is a central subject in modern condensed matter physics. Various ordered and liquid phases as well as multiferroic behavior can arise from geometric frustration. The kagome net is a well-known example of lattice geometry that exhibits a high degree of frustration. This lattice geometry is proposed to host various exotic phases such as a quantum spin liquid, valence bond solid [1–4], and the fractional quantum Hall state [5]. The intriguing feature of the kagome lattice is the nondispersing flatband arising from geometric frustration. It enhances the interaction effect and leads to ferromagnetic order [6] as well as the destruction of Bose-Einstein condensation and the resulting supersolid state [7]. Superconductivity (superfluidity) on the kagome lattice is a recent topic of great interest from the theoretical side, despite the fact that few corresponding systems are known [8]. The infinitely large density of states associated with the flatband can strongly enhance superconductivity in the kagome lattice [9]. Geometric frustration also provides a highly nontrivial effect on electron correlations and thus can lead to the emergence of novel superconducting states [10].

Ultracold atoms trapped within optical lattices offer an ideal system for exploring various exotic phases and studying quantum phase transitions due to their remarkable controllability and cleanliness [11]. The stability of superflow and critical velocity are of particular interest for Fermi and Bose superfluids in optical lattices since the pioneering experiments by Ketterle *et al.* [12]. Various dynamical instabilities arising from competing orders in optical lattices and the possibility of a “flowing supersolid” state have been investigated [13–17]. The experiments by Jo *et al.* [18] realized a tunable optical lattice in the kagome geometry by overlaying two triangular lattices with commensurate wavelengths. By introducing

fermionic isotopes <sup>6</sup>Li or <sup>40</sup>K into optical kagome lattices, this system would provide a very important platform for studying superconductivity and Cooper pairing in the kagome lattice.

In this Letter, motivated by the recent experimental developments reported by Jo *et al.* [18], we study the superfluidity of atomic fermions in an optical kagome lattice within the attractive fermion Hubbard model. Imposing a nonzero superflow, we calculate an order parameter characterizing a condensate of fermion pairs as well as fermion density within the mean-field approximation. We further study superflow instabilities which limit the critical current by evaluating the free energy as a function

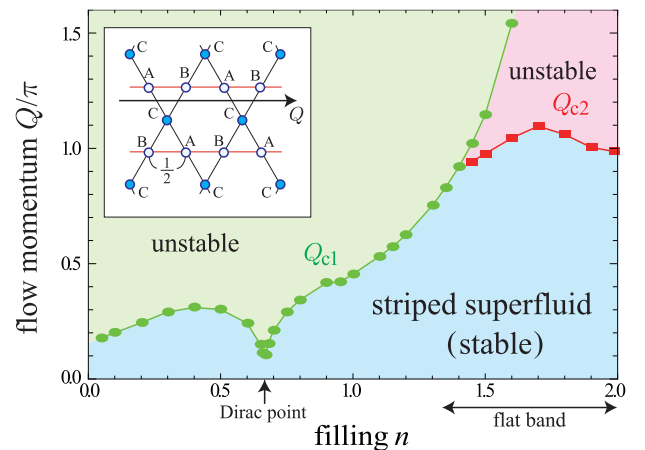


FIG. 1: (color online). Stability phase diagram of a flowing superfluid state in the kagome lattice. We set the flow momentum  $\mathbf{Q} = (Q, 0)$  and  $T = 0$ .  $Q_{c1}$  and  $Q_{c2}$  are the critical flow momenta for dynamical instabilities with distinct mechanisms (see the text). The inset shows the stripe charge order induced by superflow with  $n_A = n_B \neq n_C$  (see the text).

of the flow momentum. Figure 1 shows the stability phase diagram of an  $s$ -wave superfluid state that summarizes the main results of this Letter. We find a novel geometric effect of the kagome lattice that leads to a stable flow-induced charge modulated superfluid state where the superfluid order and charge density wave (CDW) order coexist (see the inset of Fig. 1) analogous to the “flowing supersolid” proposed in Ref. 13. Furthermore, the critical current for this state is found to be quite enhanced at high fermion density due to the diverging density of states (DOS) associated with the flatband. We also find that the instabilities at the critical current are dominated by the different mechanisms at the low and high fermion densities. The stability phase diagram thus shows a remarkable particle-hole asymmetry of the critical current. The unexpected charge modulations we uncover can be observed by employing the setup of the recent cold-atom experiments [18] combined with the moving optical lattice technique [12, 19, 20] or dipole oscillations [21]. The charge modulations induced by superflow may be also observed around a quantized vortex.

We consider two-component atomic fermions in a deep optical kagome lattice described by the attractive Hubbard model:  $\hat{H} = -t \sum_{\langle i,j \rangle, \sigma} (\hat{c}_{i\sigma}^\dagger \hat{c}_{j\sigma} + \text{h.c.}) - U \sum_i \hat{n}_{i\uparrow} \hat{n}_{i\downarrow} - \mu \sum_{i,\sigma} \hat{n}_{i\sigma}$ , where  $\hat{c}_{i\sigma}^\dagger$  creates a fermion with spin  $\sigma (= \uparrow, \downarrow)$  at site  $i$ ,  $\hat{n}_{i\sigma} = \hat{c}_{i\sigma}^\dagger \hat{c}_{i\sigma}$ ,  $t (> 0)$  is a hopping amplitude between the nearest-neighbor sites,  $U (\geq 0)$  is the local Hubbard attraction, and  $\mu$  is the chemical potential. For  $U = 0$ , we obtain the three energy bands:  $\varepsilon_0 = 2t$  and  $\varepsilon_{\pm}(\mathbf{k}) = t \left( -1 \pm \sqrt{3 + 2 \sum_{i=1,2,3} \cos(\mathbf{k} \cdot \mathbf{a}_i)} \right)$  with  $\mathbf{a}_1 = (1, 0)$ ,  $\mathbf{a}_2 = (1/2, \sqrt{3}/2)$ , and  $\mathbf{a}_3 = \mathbf{a}_2 - \mathbf{a}_1$ . The flat band  $\varepsilon_0$  is occupied if the fermion filling  $n$  is in the range of  $4/3 \leq n \leq 2$ , while the Fermi energy is at the Dirac points in  $\varepsilon_{\pm}(\mathbf{k})$  when  $n = 2/3$ .

We introduce the order parameter in the presence of superfluid flow with flow momentum  $\mathbf{Q}$  in the reference frame fixed to the lattice potential [22, 23],  $\Delta_\nu = (U/M) \sum_{\mathbf{k}} \langle \hat{c}_{-\mathbf{k}+\mathbf{Q}/2, \nu, \downarrow} \hat{c}_{\mathbf{k}+\mathbf{Q}/2, \nu, \uparrow} \rangle$ , and the average number of atoms per site,  $n_\nu = (1/M) \sum_{\mathbf{k}, \sigma} \langle \hat{c}_{\mathbf{k}, \nu, \sigma}^\dagger \hat{c}_{\mathbf{k}, \nu, \sigma} \rangle$ , where  $\hat{c}_{\mathbf{k}, \nu, \sigma}$  is the Fourier component of  $\hat{c}_{i\sigma}$ ,  $M$  is the number of unit cells, and  $\nu (= A, B, C)$  labels the sublattice as shown in the inset of Fig. 1. In the following calculation, we use the periodic boundary condition assuming that the system size is sufficiently large ( $M \gg 1$ ) so that the momentum can take continuous values. The fermion filling is given by  $n = (n_A + n_B + n_C)/3$ . Within the Hartree-Fock-Gor’kov (HFG) approximation, the Hamiltonian takes the form

$$\hat{H}_{\text{HFG}} = \sum_{\mathbf{k}} \Psi_{\mathbf{Q}}^\dagger(\mathbf{k}) \hat{h}_{\mathbf{Q}}(\mathbf{k}) \Psi_{\mathbf{Q}}(\mathbf{k}) + E_{\mathbf{Q}}^0, \quad (1)$$

with

$$\Psi_{\mathbf{Q}}^\dagger(\mathbf{k}) = (\hat{c}_{\mathbf{k}+, A, \uparrow}^\dagger \hat{c}_{\mathbf{k}-, A, \downarrow} \hat{c}_{\mathbf{k}+, B, \uparrow}^\dagger \hat{c}_{\mathbf{k}-, B, \downarrow} \hat{c}_{\mathbf{k}+, C, \uparrow}^\dagger \hat{c}_{\mathbf{k}-, C, \downarrow})$$

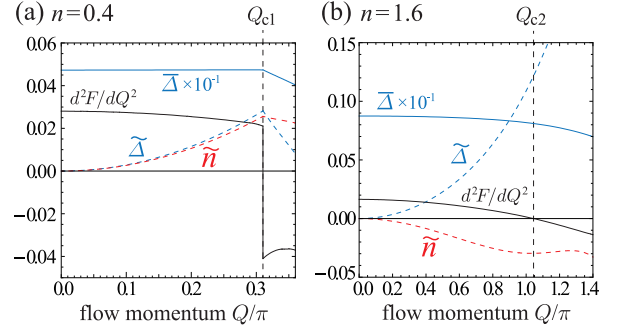


FIG. 2: (color online). Density modulation  $\tilde{n}$ , order parameter modulation  $\tilde{\Delta}$ , and averaged order parameter  $\bar{\Delta}$  as functions of flow momentum  $\mathbf{Q} = (Q, 0)$  for (a)  $n = 0.4$  and (b)  $n = 1.6$ . We set  $U/t = 3$  and  $T = 0$ .  $Q_{c1}$  and  $Q_{c2}$  are the critical flow momenta.

and  $E_{\mathbf{Q}}^0 = -3M(\mu + Un/2) + M \sum_{\nu} (|\Delta_{\nu}|^2/U + Un_{\nu}^2/4)$ . Here,  $\mathbf{k}_{\pm}$  denotes  $\pm \mathbf{k} + \mathbf{Q}/2$ . The explicit form of  $\hat{h}_{\mathbf{Q}}(\mathbf{k})$  is presented in the Supplemental Material [22]. We obtain the excitation spectrum of Bogoliubov quasiparticles  $E_{\mathbf{Q}, \tau}(\mathbf{k})$  for the energy band  $\tau (= \pm, 0)$  as the eigenvalues of the matrix  $\hat{h}_{\mathbf{Q}}(\mathbf{k})$ . To evaluate  $\Delta_{\nu}$  and  $n_{\nu}$ , we solve three gap and three number equations self-consistently in the standard manner [17]. This scheme is known to interpolate the BCS and BEC regimes at low temperatures [24].

In the stationary ground state ( $\mathbf{Q} = \mathbf{0}$ ), the order parameters as well as the filling factors take the same value for all the sublattices by the symmetry. If we impose nonzero superflow, we find that an infinitesimally small amount of superflow breaks this symmetry and leads to spatial modulations in density and order parameter. We plot  $\tilde{n} \equiv n_C - n_A$ ,  $\tilde{\Delta} \equiv \Delta_C - \Delta_A$ , and the averaged order parameter  $\bar{\Delta} \equiv (\Delta_A + \Delta_B + \Delta_C)/3$  as functions of  $Q$  for different fillings in Figs. 2(a) and 2(b) setting the flow in the  $\Gamma - K$  direction ( $\mathbf{Q} = (Q, 0)$ ). The system involves a stripe order in the direction perpendicular to the flow with  $\Delta_A = \Delta_B \neq \Delta_C$  and  $n_A = n_B \neq n_C$  (see inset of Fig. 1). This superfluid state with a stripe charge order is analogous to a supersolid state in the sense that superfluid and CDW orders coexist. Such a flow-induced charge modulated state arises due to the geometric effect that is unique to the kagome lattice, while the supersolid state arises due to the spontaneous breaking of translational symmetry.

To check the stability of the superfluid state with stripe charge order, we evaluate the quantity  $\frac{1}{N} \frac{d^2 F(Q)}{dQ^2}$  that represents phase stiffness [13], where  $N = 3M$  is the number of total lattice sites and  $F(Q)$  is the free energy of the system in the presence of superflow. If this value is negative, the system is dynamically unstable against phase and density fluctuations [13, 14] so that the critical momentum of superflow is given by the value of  $Q$  at which  $\frac{dF(Q)}{dQ}$  takes the maximum [25]. Note that the su-

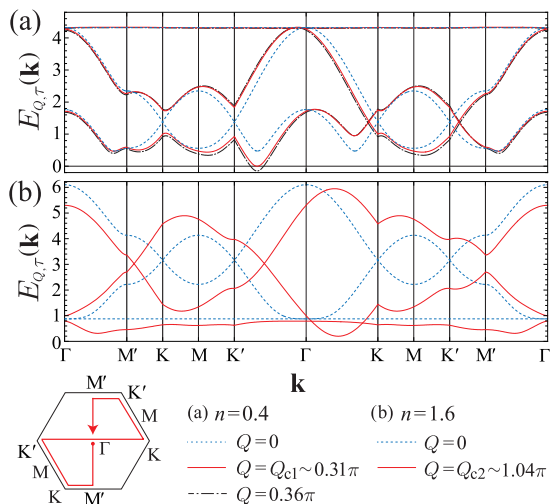


FIG. 3: (color online). Quasiparticle energy band  $E_{Q,\tau}(\mathbf{k})$  ( $\tau = 0, \pm$ ) for different values of imposed flow  $\mathbf{Q} = (Q, 0)$  at (a)  $n = 0.4$  and (b)  $n = 1.6$ . We set  $U/t = 3$  and  $T = 0$ .

perfluid density is proportional to  $d^2F(Q)/dQ^2|_{Q=0}$ . In Figs. 2(a) and 2(b),  $\frac{1}{N} \frac{d^2F(Q)}{dQ^2}$  is positive for both the low and high fillings until the critical flow momentum  $Q_{c1}$  or  $Q_{c2}$ . Consequently, the superfluid state with the stripe charge order is dynamically stable until  $Q_{c1}$  or  $Q_{c2}$ . This is in sharp contrast with the “flowing supersolid” state in a square lattice [14], which is found to be dynamically unstable with negative  $\frac{1}{N} \frac{d^2F(Q)}{dQ^2}$  for any nonzero  $Q$ .

We find that the dynamical instabilities are caused by different mechanisms for low and high fillings. The value of  $\frac{1}{N} \frac{d^2F(Q)}{dQ^2}$  in Fig. 2(a) changes discontinuously at the critical momentum  $Q_{c1}$ , while the curve in Fig. 2(b) smoothly changes from positive to negative at  $Q_{c2}$ . We find that the sudden change of the curve at  $Q_{c1}$  is associated with gapless quasiparticle excitations. With increasing flow, the energy gap to creating quasiparticles decreases due to a Doppler shift in the direction opposite to  $\mathbf{Q}$  as shown in Fig. 3 (a). For large  $Q$ , the gap closes and the lowest quasiparticle energy band  $E_{Q,\tau}(\mathbf{k})$  becomes gapless. This precisely coincides with  $Q_{c1}$ . Since the free energy at  $T = 0$  involves the contribution from spontaneously excited quasiparticles with negative energies above the critical flow  $Q \geq Q_{c1}$ , the second derivative of the free energy  $\frac{1}{N} \frac{d^2F(Q)}{dQ^2}$  changes discontinuously at  $Q = Q_{c1}$ . On the other hand, in Fig. 2(b), the quasiparticle dispersion is still gapped at  $Q_{c2}$ . Thus, the instability at  $Q_{c2}$  sets in before the closing of the single-particle excitation gap. The negative value of  $\frac{1}{N} \frac{d^2F(Q)}{dQ^2}$  therefore indicates the dynamical instability associated with collective phonon excitations rather than single-particle excitations [13, 26–28]. At the onset of the instabilities at  $Q_{c1}$  and  $Q_{c2}$ , the frequency of long-wavelength phonons becomes complex. As a result, the amplitude of collec-

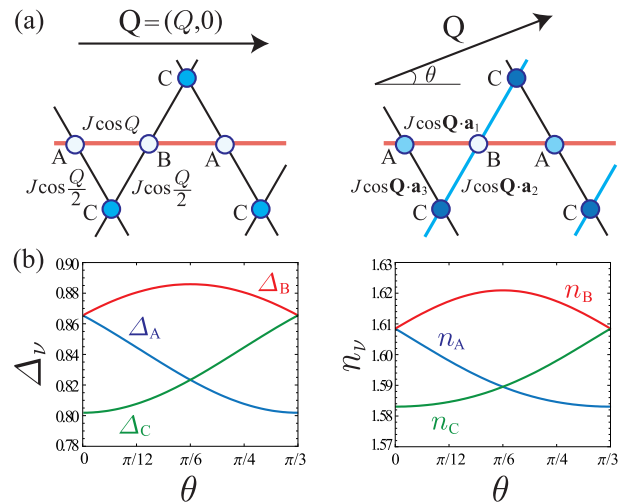


FIG. 4: (color online). (a) Effective hopping amplitudes for fermion pairs in the strong coupling regime when  $\mathbf{Q} = (Q, 0)$  and  $\mathbf{Q} = (Q \cos \theta, Q \sin \theta)$ . (b) Order parameter  $\Delta_\nu$  and fermion filling  $n_\nu$  as functions of the angle  $\theta$  defined in (b). We set  $Q = 0.8\pi$ ,  $n = 1.6$ , and  $U/t = 3$ .

tive phonon excitations grows exponentially and the superfluid state collapses.

The stability phase diagram in Fig. 1 exhibits a remarkable particle-hole asymmetry reflecting the different features of  $\frac{1}{N} \frac{d^2F(Q)}{dQ^2}$  at  $Q_{c1}$  and  $Q_{c2}$  discussed above. The critical momentum at high filling ( $n \gtrsim 4/3$ ) is significantly enhanced while being limited by the onset of the dynamical instability at  $Q_{c2}$ . The robust superfluidity against the imposed superflow is due to the flatband in the noninteracting band structure. The diverging DOS at the flatband enhances the order parameter and the single-particle energy gap. The large energy gap suppresses the depairing instability since a large Doppler shift is required for closing the gap. On the other hand, the small order parameter for low filling yields the small energy gap in Fig. 3. The dynamical instability at  $Q_{c1}$  for low filling ( $n \lesssim 4/3$ ) is therefore preempted by the closing of the single-particle excitation gap.

We now discuss the reason for the emergence of the flow-induced charge modulations. To make the argument simpler, it is convenient to describe the system in the rest frame of the condensate where the lattice potential is moving with the velocity  $\mathbf{v} = -\mathbf{Q}/2m$  [23] and we restrict ourselves within the strong coupling regime ( $U \gg t$ ) where fermion pairs become tightly bound molecular bosons. In this regime, the hopping term of the effective Hamiltonian for bosons in the presence of superflow  $\mathbf{Q}$  is given by  $-J \sum_{\langle i,j \rangle} (e^{-i\mathbf{Q} \cdot \mathbf{r}_{ij}} b_i^\dagger b_j + \text{H.c.})$ . Here,  $J = 2t^2/U$ ,  $b_i = \hat{c}_{i\downarrow} \hat{c}_{i\uparrow}$  is an annihilation operator for a boson, and  $\mathbf{r}_{ij} = \mathbf{r}_i - \mathbf{r}_j$  is the bond vector. The Hamiltonian shows that the imposed superflow reduces the effective hopping amplitude of bosons by a factor of  $\cos \mathbf{Q} \cdot \mathbf{r}_{ij}$ , which plays a crucial role for the spatial mod-

ulation. The kagome lattice has three kinds of nearest-neighbor bonds connecting two sites: the  $A$ - $B$ ,  $B$ - $C$ , and  $C$ - $A$  bonds. The flow breaks the symmetry of the three bonds and introduces the anisotropy in the hopping amplitude, which naturally leads to the spatial modulation in density and order parameter. For example, when the flow is in the  $\Gamma \rightarrow K$  direction, the effective hopping amplitudes are given by  $J_{AB} = J \cos Q$  for the  $A$ - $B$  bond and  $J_{BC} = J_{CA} = J \cos \frac{Q}{2}$  for the  $B$ - $C$  and  $C$ - $A$  bonds as shown in Fig. 4(a). Because of this anisotropy, the system prefers forming a stripe modulation with  $n_A = n_B \neq n_C$  and  $\Delta_A = \Delta_B \neq \Delta_C$  in order to maximize the energy gain. Figure 4(b) shows  $\Delta_\nu$  and  $n_\nu$  as functions of the angle  $\theta$  of the flow momentum  $\mathbf{Q}$  relative to the  $x$  axis. In general,  $\Delta_\nu$  and  $n_\nu$  take different values depending on sublattices  $A$ ,  $B$ , and  $C$  due to the anisotropy of the effective hopping amplitudes of pairs, except for some special symmetric points,  $\theta = 0, \pi/6, \pi/3, \dots$ , where two of them are equivalent and the system forms a stripe pattern. This spatial modulation obviously emerges from the characteristic geometry of the kagome lattice and therefore it is absent in other typical lattice geometries such as a square [14, 15], cubic [14, 15], honeycomb [17], and even triangular lattice that has geometric frustration.

For realizing a Fermi superfluid in optical lattices, experimental difficulties arise in cooling the system down to the superfluid transition temperature. The kagome lattice has a great advantage in this respect. The mean-field transition temperature  $T_c^0$  in Fig. 5(a) is significantly enhanced for high filling  $n \gtrsim 4/3$  when the Fermi level reaches the flatband. Despite the fact that a pure 2D system has no real condensate of pairs at finite temperatures [31],  $T_c^0$  is useful for estimating the Kosterlitz-Thouless transition temperature  $T_{KT}$  [32] in the case of  $T_F \gg T_c^0$ , i.e.,  $(T_c^0 - T_{KT})/T_c^0 \sim (T_c^0/T_F) \ll 1$  [33, 34].  $T_c^0$  also provides a good estimate for the actual transition temperature  $T_c$  of fermions in weakly coupled layers of kagome lattices in which phase fluctuation that destroys condensate is suppressed due to the inter-layer Josephson coupling while the system maintains two-dimensional features. Such a system can be realized by loading fermions into a series of pancake-shaped potentials [35] together with kagome optical lattices as realized in Ref. 18. Figure 5(b) shows that the stripe charge order is observable up to high temperatures slightly below  $T_c^0$ . We note that the curve for  $T_c^0$  in Fig. 5(a) shows a dip in the vicinity of  $n = 2/3$  due to the Dirac points in the free fermion band structure [17, 29, 30]. The system remains in the normal semimetallic phase for small  $U$  less than the critical value  $U_c \approx 2.8t$ .

The flow-induced charge modulations that we uncovered can be realized in cold-atom experiments if superflow is imposed by a moving optical lattice [12, 19, 20]. The experiment in Ref. 18 overlays two triangular lattices to form the kagome lattice. Each triangular lattice is formed by three lasers at angles of 120 degrees

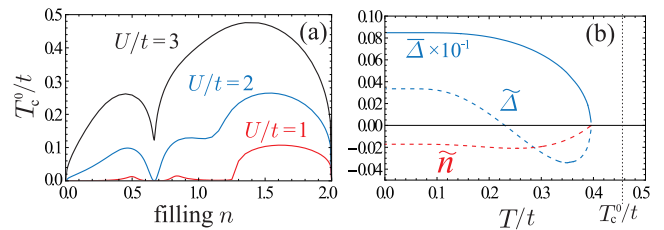


FIG. 5: (color online) (a) Mean-field transition temperature  $T_c^0$  as a function of fermion filling  $n$ . (b) Temperature dependence of  $\tilde{\Delta}$ ,  $\tilde{n}$ , and  $\tilde{\Delta}$  for  $n = 1.6$ ,  $\mathbf{Q} = (0.6\pi, 0)$ , and  $U/t = 3$ . The vertical dotted line marks  $T_c^0$  in the absence of flow.

with respect to each other. Superflow can be induced in the  $\Gamma - K$  direction by detuning one of the lasers for each triangular lattice and moving both the triangular lattices with the same velocity [22]. Superflow can be also imposed by dipole oscillations which can be induced by a sudden displacement of a confining harmonic potential [21]. Since infinitesimally small flow can induce charge modulations, superflow around a single vortex induces charge modulations that extend over the whole system; therefore, it may also be easily observed.

In summary, we have studied the  $s$ -wave superfluid state of atomic fermions on the kagome lattice inspired by the recent realization of tunable kagome optical lattices [18]. We performed a mean-field analysis of the superfluid state imposing superflow. We found that superflow induces a novel charge modulated state due to the characteristic geometry of the kagome lattice. The superfluid and CDW orders coexist in this state analogous to the “supersolid” state. We examined the superflow instabilities and critical current by evaluating the free energy as a function of superflow. The critical current for high filling was found to be quite enhanced due to the flatband in the free fermion band structure. The superfluid state with charge modulations sustains high temperatures close to the mean-field transition temperature  $T_c^0$  which is also enhanced by the flat band for high filling and therefore accessible using the setup that is realizable in cold-atom experiments.

We acknowledge T. Ohkane for performing preliminary calculations in the early stage of this work. S. T. and D. Y. were supported by a Grant-in-Aid for Scientific Research, Grants No. 24740276 (S. T.) and No. 23840054 (D. Y.).

- 
- [1] V. Elser, Phys. Rev. Lett. **62**, 2405 (1989).
  - [2] J. B. Masrston and C. Zeng, J. Appl. Phys. **69**, 5962 (1991).
  - [3] S. Sachdev, Phys. Rev. B **45**, 12377 (1992).
  - [4] L. Balents, Nature (London), **464**, 199 (2010).
  - [5] E. Tang, J.-W. Mei, and X.-G. Wen, Phys. Rev. Lett. **106**,

- 236802 (2011).
- [6] H. Tasaki, Phys. Rev. Lett. **69**, 1608 (1992); A. Mielke, J. Phys. A **24**, 3311 (1991).
- [7] S. D. Huber and E. Altman, Phys. Rev. B **82**, 184502 (2010).
- [8] M. Kiesel, C. Platt, and R. Thomale, arXiv:1209.3398.
- [9] M. Imada and M. Kohno, Phys. Rev. Lett. **84**, 143 (2000).
- [10] Z. Hiroi and M. Ogata, *Introduction to Frustrated Magnetism*, Springer Series in Solid State Sciences Vol. 164 (Springer-Verlag, Berlin, 2011).
- [11] I. Bloch, J. Dalibard, and W. Zwerger, Rev. Mod. Phys. **80**, 885 (2008).
- [12] J. Mun, P. Medley, G. K. Campbell, L. G. Marcassa, D. E. Pritchard, and W. Ketterle, Phys. Rev. Lett. **99**, 150604 (2007).
- [13] A. A. Burkov and A. Paramekanti, Phys. Rev. Lett. **100**, 255301 (2008).
- [14] R. Ganesh, A. Paramekanti, and A. A. Burkov, Phys. Rev. A **80**, 043612 (2009).
- [15] Y. Yunomae, D. Yamamoto, I. Danshita, N. Yokoshi, and S. Tsuchiya, Phys. Rev. A **80**, 063627 (2009).
- [16] I. Danshita and D. Yamamoto, Phys. Rev. A **82**, 013645 (2010).
- [17] S. Tsuchiya, R. Ganesh, and A. Paramekanti, Phys. Rev. A **86**, 033604 (2012).
- [18] G.-B. Jo, J. Guzman, C. K. Thomas, P. Hosur, A. Vishwanath, and D. M. Stamper-Kurn, Phys. Rev. Lett. **108**, 045305 (2012).
- [19] D. E. Miller, J. K. Chin, C. A. Stan, Y. Liu, W. Setiawan, C. Sanner, and W. Ketterle, Phys. Rev. Lett. **99**, 070402 (2007).
- [20] L. Fallani, L. De Sarlo, J. E. Lye, M. Modugno, R. Saers, C. Fort, and M. Inguscio, Phys. Rev. Lett. **93**, 140406 (2004).
- [21] S. Burger, F. S. Cataliotti, C. Fort, F. Minardi, M. Inguscio, M. L. Chiofalo, and M. P. Tosi, Phys. Rev. Lett. **86**, 4447 (2001); C. D. Fertig, K. M. O'Hara, J. H. Huckans, S. L. Rolston, W. D. Phillips, and J. V. Porto, Phys. Rev. Lett. **94**, 120403 (2005).
- [22] See Supplemental Material attached below for details.
- [23] The effect of superfluid flow can be introduced either by imposing a phase gradient on the fermion operator or by imposing pair formation with a finite center-of-mass momentum as in the text. We prove the equivalence of them in Sec. C of the Supplemental Material [22].
- [24] A. J. Leggett, *Modern Trends in the Theory of Condensed Matter* (Springer, Berlin, 1980).
- [25] L. Goren and E. Altman, Phys. Rev. Lett. **104**, 257002 (2010).
- [26] M. Machholm, C. J. Pethick, and H. Smith, Phys. Rev. A **67**, 053613 (2003).
- [27] E. Taylor and E. Zaremba, Phys. Rev. A **68**, 053611 (2003).
- [28] L. P. Pitaevskii, S. Stringari, and G. Orso, Phys. Rev. A **71**, 053602 (2005).
- [29] E. Zhao and A. Paramekanti, Phys. Rev. Lett. **97**, 230404 (2006).
- [30] K. L. Lee, B. Grémaud, R. Han, B.-G. Englert, and C. Miniatura, Phys. Rev. A **80**, 043411 (2009).
- [31] N. D. Mermin and H. Wagner, Phys. Rev. Lett. **17**, 1133 (1966).
- [32] J. M. Kosterlitz and D. J. Thouless, J. Phys. C **6**, 1181 (1973).
- [33] K. Miyake, Prog. Theor. Phys. **69**, 1794 (1983).
- [34] G. Orso and G. V. Shlyapnikov, Phys. Rev. Lett. **95**, 260402 (2005).
- [35] K. Martiyanov, V. Makhalov, and A. Turlapov, Phys. Rev. Lett. **105**, 030404 (2010).

## Supplementary Material for “Flow-Induced Spatial Modulation of Superfluid Atomic Fermions in an Optical Kagome Lattice”

### A. The explicit form of $\hat{h}_{\mathbf{Q}}(\mathbf{k})$

The explicit form of the  $6 \times 6$  matrix  $\hat{h}_{\mathbf{Q}}(\mathbf{k})$  in Eq. (1) of the main text is given by

$$\hat{h}_{\mathbf{Q}} = \begin{pmatrix} -\mu - \frac{U}{2}n_A & -\Delta_A & -2t \cos(\mathbf{k}_+ \cdot \frac{\mathbf{a}_1}{2}) & 0 & -2t \cos(\mathbf{k}_+ \cdot \frac{\mathbf{a}_3}{2}) & 0 \\ -\Delta_A^* & \mu + \frac{U}{2}n_A & 0 & 2t \cos(\mathbf{k}_- \cdot \frac{\mathbf{a}_1}{2}) & 0 & 2t \cos(\mathbf{k}_- \cdot \frac{\mathbf{a}_3}{2}) \\ -2t \cos(\mathbf{k}_+ \cdot \frac{\mathbf{a}_1}{2}) & 0 & -\mu - \frac{U}{2}n_B & -\Delta_B & -2t \cos(\mathbf{k}_+ \cdot \frac{\mathbf{a}_2}{2}) & 0 \\ 0 & 2t \cos(\mathbf{k}_- \cdot \frac{\mathbf{a}_1}{2}) & -\Delta_B^* & \mu + \frac{U}{2}n_B & 0 & 2t \cos(\mathbf{k}_- \cdot \frac{\mathbf{a}_2}{2}) \\ -2t \cos(\mathbf{k}_+ \cdot \frac{\mathbf{a}_3}{2}) & 0 & -2t \cos(\mathbf{k}_+ \cdot \frac{\mathbf{a}_2}{2}) & 0 & -\mu - \frac{U}{2}n_C & -\Delta_C \\ 0 & 2t \cos(\mathbf{k}_- \cdot \frac{\mathbf{a}_3}{2}) & 0 & 2t \cos(\mathbf{k}_- \cdot \frac{\mathbf{a}_2}{2}) & -\Delta_C^* & \mu + \frac{U}{2}n_C \end{pmatrix}.$$

The matrix  $\hat{h}_{\mathbf{Q}}$  can be diagonalized by the Bogoliubov transformation in the standard manner [1]. Without imposed superflow, we can take  $\Delta_A = \Delta_B = \Delta_C \equiv \Delta$  and  $n_A = n_B = n_C \equiv n$  due to the symmetry of the lattice. In this case,  $\hat{h}_{\mathbf{Q}}$  can be analytically diagonalized to give the gap and number equations

$$\frac{\Delta}{U} = \frac{1}{N} \sum_{\mathbf{k}} \sum_{\tau=0,\pm} \frac{\Delta}{2E_{\mathbf{Q}=0,\tau}(\mathbf{k})} \tanh \frac{\beta E_{\mathbf{Q}=0,\tau}(\mathbf{k})}{2} \quad (2)$$

and

$$n = 1 - \frac{1}{N} \sum_{\mathbf{k}} \sum_{\tau=0,\pm} \frac{\xi_{\tau}(\mathbf{k})}{E_{\mathbf{Q}=0,\tau}(\mathbf{k})} \tanh \frac{\beta E_{\mathbf{Q}=0,\tau}(\mathbf{k})}{2}, \quad (3)$$

respectively. Here,  $N = 3M$  is the number of total lattice sites,  $\beta = 1/T$  is the inverse temperature, and  $\xi_\tau(\mathbf{k}) = \varepsilon_\tau(\mathbf{k}) - \mu - Un/2$ . The Bogoliubov quasiparticle bands for  $\mathbf{Q} = \mathbf{0}$  are simply given by  $E_{\mathbf{Q}=\mathbf{0},\tau}(\mathbf{k}) = \sqrt{\xi_\tau(\mathbf{k})^2 + |\Delta|^2}$ . There exists one flat band ( $\tau = 0$ ) even in the superfluid state (see Fig. 3 of the main text).

### B. Moving kagome optical lattice

We present here how to prepare a *moving* optical lattice with kagome geometry. In the recent experiment by Jo *et al.* [2], the kagome lattice was formed by overlaying two triangular optical lattices with different lattice constants. Therefore, we only have to consider the setup for moving a triangular-lattice potential with a constant velocity. The triangular lattice is generated by superposing three laser beams that intersect in the  $x$ - $y$  plane with wave vectors  $\mathbf{k}_1 = k(1, 0)$ ,  $\mathbf{k}_2 = k(-1/2, -\sqrt{3}/2)$ , and  $\mathbf{k}_3 = k(-1/2, \sqrt{3}/2)$ . All beams are linearly polarized orthogonal to the plane and have the same field strength  $E_0$ . The total electric field is given by

$$\mathbf{E}(\mathbf{r}, t) = \sum_{i=1}^3 E_0 \cos(\mathbf{k}_i \cdot \mathbf{r} - \omega t + \phi_i) \mathbf{e}_z. \quad (4)$$

The relative phases  $\phi_{ij} = \phi_i - \phi_j$  are fixed in Ref. 2 to obtain a stable optical lattice. The generated dipole potential is proportional to the squared amplitude of the electric field

$$\begin{aligned} |\mathbf{E}_{\text{tot}}|^2 = \frac{E_0^2}{2} & \left[ 3 + 2 \cos(\mathbf{b}_1 \cdot \mathbf{r} + \phi_{23}) + 2 \cos(\mathbf{b}_2 \cdot \mathbf{r} + \phi_{31}) + 2 \cos(\mathbf{b}_3 \cdot \mathbf{r} + \phi_{12}) \right. \\ & + \cos(2\mathbf{k}_1 \cdot \mathbf{r} - 2\omega t + 2\phi_1) + \cos(2\mathbf{k}_2 \cdot \mathbf{r} - 2\omega t + 2\phi_2) + \cos(2\mathbf{k}_3 \cdot \mathbf{r} - 2\omega t + 2\phi_3) \\ & + 2 \cos((\mathbf{k}_2 + \mathbf{k}_3) \cdot \mathbf{r} - 2\omega t + \phi_2 + \phi_3) + 2 \cos((\mathbf{k}_3 + \mathbf{k}_1) \cdot \mathbf{r} - 2\omega t + \phi_3 + \phi_1) \\ & \left. + 2 \cos((\mathbf{k}_1 + \mathbf{k}_2) \cdot \mathbf{r} - 2\omega t + \phi_1 + \phi_2) \right], \end{aligned} \quad (5)$$

where  $\mathbf{b}_i = \varepsilon_{ijk}(\mathbf{k}_j - \mathbf{k}_k)$ . Since the frequency of light is quite large, only the time-averaged value of  $|\mathbf{E}_{\text{tot}}|^2$  can affect atoms. Therefore, by dropping the terms containing  $2\omega t$ , we obtain a periodic dipole potential

$$V(\mathbf{r}) = V_0 \left( \frac{3}{2} + \cos(\mathbf{b}_1 \cdot \mathbf{r} + \phi_{23}) + \cos(\mathbf{b}_2 \cdot \mathbf{r} + \phi_{31}) + \cos(\mathbf{b}_3 \cdot \mathbf{r} + \phi_{12}) \right). \quad (6)$$

Red-detuned lasers give  $V_0 < 0$  and we obtain a regular triangular-lattice potential, while the maxima of  $V(\mathbf{r})$  form a triangular lattice in the case of blue-detuned lasers ( $V_0 > 0$ ) [3]. Therefore, we can cancel out unwanted sites of a triangular lattice with  $V_0 < 0$  by overlaying another potential with  $V_0 > 0$  so that the total potential minima form a kagome lattice [2].

One can move the lattice potential by introducing time-dependent phase differences  $\phi_{ij}(t)$  through a small frequency detuning  $\delta\omega$ . Let us say that we detune one of the three lasers making a triangular lattice as  $\phi_1 = \delta\omega t$  and  $\phi_2 = \phi_3 = 0$ . In this case, we can rewrite Eq. (6) as

$$\begin{aligned} V(\mathbf{r}) &= V_0 \left( \frac{3}{2} + \cos(\mathbf{b}_1 \cdot \mathbf{r}) + \cos(\mathbf{b}_2 \cdot \mathbf{r} - \delta\omega t) + \cos(\mathbf{b}_3 \cdot \mathbf{r} + \delta\omega t) \right) \\ &= V_0 \left( \frac{3}{2} + \cos(\sqrt{3}ky) + 2 \cos\left(\frac{3}{2}k \left(x + \frac{2\delta\omega}{3k}t\right)\right) \cos\left(\frac{\sqrt{3}}{2}ky\right) \right), \end{aligned} \quad (7)$$

which means that the potential moves in the  $\Gamma$ - $K$  direction with a constant velocity  $2\delta\omega/3k$ . A moving kagome optical lattice can be obtained by moving both the overlaid triangular lattices with a same velocity. Note that one uses two sets of lasers with different values of  $k$  to create a kagome lattice [2]. Therefore, the frequency detuning  $\delta\omega$  of each triangular-lattice potential has to be tuned so that the velocities  $2\delta\omega/3k$  take a same value.

### C. Effect of a moving optical lattice

We show that the effect of a moving optical lattice in the laboratory frame can be properly described by imposing pair formation with nonzero center-of-mass momentum in the frame moving with the lattice potential. In the following argument, we assume a square optical lattice for simplicity. Its extension to multiple-sublattice geometries is straightforward.

Let us start with the standard attractive Hubbard model:@

$$\hat{H} = -t \sum_{\langle i,j \rangle, \sigma} \left( \hat{c}_{i\sigma}^\dagger \hat{c}_{j\sigma} + \text{h.c.} \right) - U \sum_i \hat{n}_{i\uparrow} \hat{n}_{i\downarrow} - \mu \sum_{i,\sigma} \hat{n}_{i\sigma}. \quad (8)$$

In the laboratory frame  $\Sigma'$ , the effect of the lattice potential moving with a constant velocity  $\mathbf{v}$  can be conveniently taken into account by the transformation that imposes a phase gradient on the fermion operator  $\hat{c}_{i\sigma} \rightarrow \hat{c}'_{i\sigma} e^{-im\mathbf{v}\cdot\mathbf{r}_i}$  [4], and the Hamiltonian can be written as

$$\begin{aligned} \hat{H}' &= -t \sum_{\langle i,j \rangle, \sigma} \left( e^{-i\mathbf{Q}\cdot\mathbf{r}_{ij}/2} \hat{c}'_{i\sigma} \hat{c}'_{j\sigma} + \text{h.c.} \right) - U \sum_i \hat{n}'_{i\uparrow} \hat{n}'_{i\downarrow} - \mu \sum_{i,\sigma} \hat{n}'_{i\sigma} \\ &= \sum_{\mathbf{k}, \sigma} \varepsilon_{\mathbf{k}+\mathbf{Q}/2} \hat{c}'_{\mathbf{k}\sigma} \hat{c}'_{\mathbf{k}\sigma} - U \sum_i \hat{n}'_{i\uparrow} \hat{n}'_{i\downarrow} - \mu \sum_{i,\sigma} \hat{n}'_{i\sigma}, \end{aligned} \quad (9)$$

where  $\mathbf{Q} = -2m\mathbf{v}$  and  $\varepsilon_{\mathbf{k}} = -2t(\cos k_x + \cos k_y)$ . In the stationary state, since the condensate can coherently transport through the lattice potential, the condensate is at rest in the laboratory frame and consequently pairs have zero center-of-mass momentum

$$\Delta' = U \langle \hat{c}'_{i\downarrow} \hat{c}'_{i\uparrow} \rangle = \frac{U}{M} \sum_{\mathbf{k}} \langle \hat{c}'_{-\mathbf{k},\downarrow} \hat{c}'_{\mathbf{k},\uparrow} \rangle. \quad (10)$$

As a result, the Hamiltonian within the Hartree-Fock-Gor'kov (HFG) mean-field approximation takes the form

$$\hat{H}'_{\text{HFG}} = \sum_{\mathbf{k}} (c'_{\mathbf{k},\uparrow}^\dagger, c'_{-\mathbf{k},\downarrow}) \begin{pmatrix} \tilde{\xi}_{\mathbf{k}+\mathbf{Q}/2} & -\Delta' \\ -\Delta' & -\tilde{\xi}_{-\mathbf{k}+\mathbf{Q}/2} \end{pmatrix} \begin{pmatrix} c'_{\mathbf{k},\uparrow} \\ c'_{-\mathbf{k},\downarrow}^\dagger \end{pmatrix}, \quad (11)$$

where  $\tilde{\xi}_{\mathbf{k}} = \varepsilon_{\mathbf{k}} - \mu - Un/2$ .

On the other hand, in the frame  $\Sigma$  moving with the optical lattice potential, the stationary state described above is equivalent to the condensate carrying finite flow momentum  $\mathbf{Q}$  described by the order parameter

$$\Delta e^{i\mathbf{Q}\cdot\mathbf{r}_i} = U \langle \hat{c}_{i\downarrow} \hat{c}_{i\uparrow} \rangle = e^{i\mathbf{Q}\cdot\mathbf{r}_i} \frac{U}{M} \sum_{\mathbf{k}} \langle \hat{c}_{-\mathbf{k}+\mathbf{Q}/2,\downarrow} \hat{c}_{\mathbf{k}+\mathbf{Q}/2,\uparrow} \rangle. \quad (12)$$

Within the HFG mean-field approximation, the Hamiltonian (8) takes the form

$$\hat{H}_{\text{HFG}} = \sum_{\mathbf{k}} (c_{\mathbf{k}+\mathbf{Q}/2,\uparrow}^\dagger, c_{-\mathbf{k}+\mathbf{Q}/2,\downarrow}) \begin{pmatrix} \tilde{\xi}_{\mathbf{k}+\mathbf{Q}/2} & -\Delta \\ -\Delta & -\tilde{\xi}_{-\mathbf{k}+\mathbf{Q}/2} \end{pmatrix} \begin{pmatrix} c_{\mathbf{k}+\mathbf{Q}/2,\uparrow} \\ c_{-\mathbf{k}+\mathbf{Q}/2,\downarrow}^\dagger \end{pmatrix}, \quad (13)$$

In the paper, we set up flow in the frame  $\Sigma$  imposing pair formation with nonzero center-of-mass momentum as in Eq. (12).

The mean-field Hamiltonians in Eqs. (11) and (13) as well as the order parameters in Eqs. (10) and (12) are equivalent under the shift of the origin of momentum of the operators:  $\hat{c}'_{\mathbf{k},\sigma} \leftrightarrow \hat{c}_{\mathbf{k}+\mathbf{Q}/2,\sigma}$ . This shows that the effect of the moving optical lattice in the frame  $\Sigma'$  can be properly described by imposing pair formation with nonzero center-of-mass momentum  $\mathbf{Q}$  in the frame  $\Sigma$ .

- 
- [1] S. Tsuchiya, R. Ganesh, and A. Paramekanti, Phys. Rev. A **86**, 033604 (2012).  
[2] G.-B. Jo, J. Guzman, C. K. Thomas, P. Hosur, A. Vishwanath, and D. M. Stamper-Kurn, Phys. Rev. Lett. **108**, 045305 (2012).  
[3] K. L. Lee, B. Grémaud, R. Han, B.-G. Englert, and C. Miniatura, Phys. Rev. A **80**, 043411 (2009).  
[4] L. P. Pitaevskii, S. Stringari, and G. Orso, Phys. Rev. A **71**, 053602 (2005).